Theoretical Investigation of Unimolecular Decomposition Channels of Furan4*

RUIFENG LIU, XUEFENG ZHOU, LEI ZHAI
Department of Chemistry, East Tennessee State University, Johnson City, Tennessee 37614-0695

Received 7 June 1997; accepted 29 August 1997

ABSTRACT: Density functional theory and high-level *ab initio* calculations were carried out to investigate three unimolecular decomposition channels of furan. All equilibrium and transition state structures along the proposed decomposition channels are fully optimized by B3LYP/6-31G** and characterized at the same level of theory by vibrational and intrinsic reaction coordinate analyses. Relative energies of the optimized structures were evaluated at theoretical levels up to QCISD(T)/6-311++G**. The theoretical results suggest that the unimolecular decomposition channel of isoxazole, proposed in an experimental study and implied to be the main decomposition channel of furan, is responsible only for the formation of $HC{\equiv}CH$ and $H_2O{=}C{=}O$, minor products of furan thermal decomposition. A new decomposition mechanism, proposed in the present study, is shown to be more likely responsible for the formation of $CH_3C{\equiv}CH$ and CO, major products of furan thermal decomposition. © 1998 John Wiley & Sons, Inc. *J Comput Chem* **19**: 240–249, 1998

Keywords: furan; decomposition mechanism; *ab initio*; DFT

Introduction

Because of the change in fuel sources such as coals and shell oil, fuels of the future will tend to have more aromatic contents.[1] Although much effort has been devoted to the study of pyrolysis and oxidation of aliphatic and aromatic hydrocarbons, very little has been done to elucidate the decomposition mechanisms and kinetics of five-membered heterocyclic compounds at combustion temperatures. This fact contrasts with the widespread natural occurrence of these species and the growing recognition of their roles in several areas such as air pollution,[2] petroleum refining, and coal liquefaction and gasification processes.[3] In an effort to understand the pyrolysis pattern of

*This article is dedicated to Prof. Norman L. Allinger.

Correspondence to: R. Liu; e-mail: liur@etsu.east-tenn-st.edu

Contract/grant sponsors: Research and Development Committee of East Tennessee State University; Cottrel College Science Award

CCC 0192-8651 / 98 / 020240-10

five-membered cyclic ethers, Lifshitz et al.[4] studied thermal decomposition of furan behind reflected shocks in a single shock tube over the temperature range 1050−1460 K. Major decomposition products were identified as methylacetylene, carbon monoxide, and acetylene. Methylacetylene and carbon monoxide were suggested to be produced by a unimolecular reaction channel, furan → $CH_3C{\equiv}CH + CO$. Acetylene was suggested to be produced through a second unimolecular channel, furan → $HC{\equiv}CH + H_2C{=}C{=}O$. However, mechanistic details of these channels were not discussed in the experimental study.[4]

In a later, more detailed study of isoxazole thermal decomposition,[5] acetonitrile (CH_3CN) and carbon monoxide were identified as the major products followed by hydrogen cyanide and several minor products. On the basis of a detailed computer modeling, production of CH_3CN, CO, and HCN was proposed to be unimolecular and to follow the mechanism[5] described in Scheme 1. It was also implied that pyrolysis of furan to produce $CH_3C{\equiv}CH$, CO, and $HC{\equiv}CH$ follows a similar mechanism.[5]

Our recent theoretical study[6] of isoxazole thermal decomposition indicates, however, that the mechanism of Scheme 1 is responsible for the formation of HCN (minor product) only. The decomposition channel described in Scheme 2 was shown to be more likely responsible for the formation of CH_3CN and CO (major products).[6]

Because furan is isoelectron with isoxazole, it is reasonable to believe that both the mechanisms described in Schemes 3 and 4 may be operative for thermal decomposition of furan. In addition, Scheme 5 is also a reasonable unimolecular decomposition channel for furan.

To understand the pyrolysis patterns of five-membered heterocyclic aromatic compounds, we performed a detailed theoretical investigation of

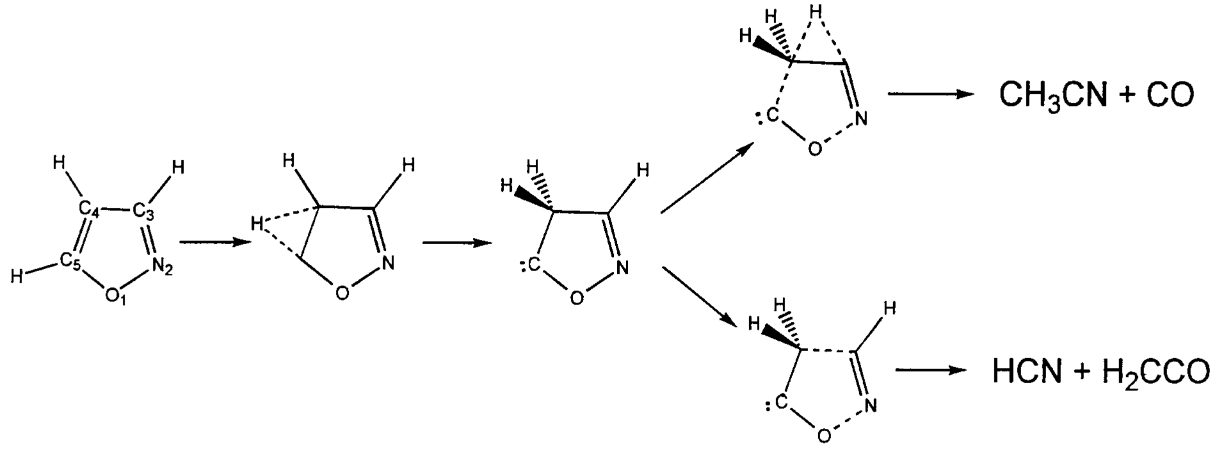

SCHEME 1

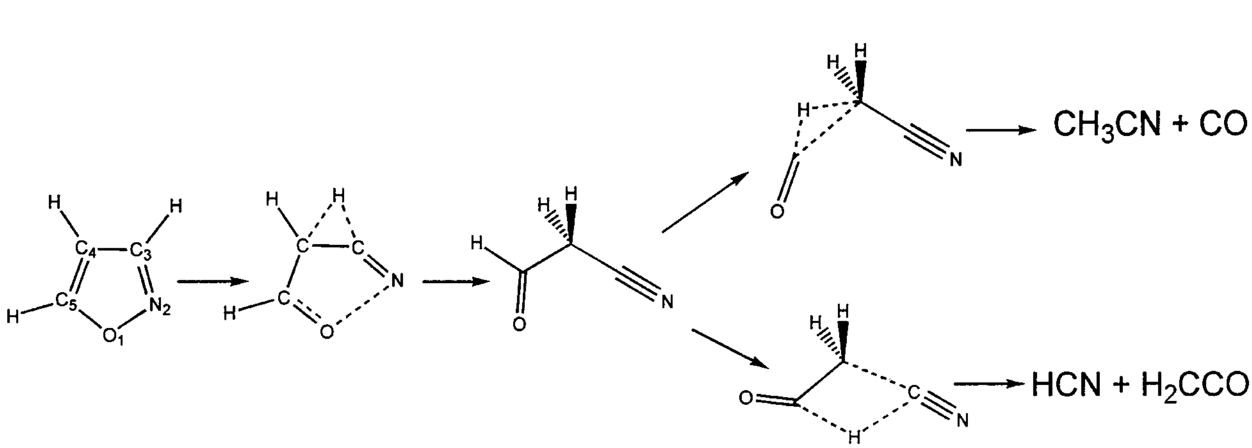

SCHEME 2

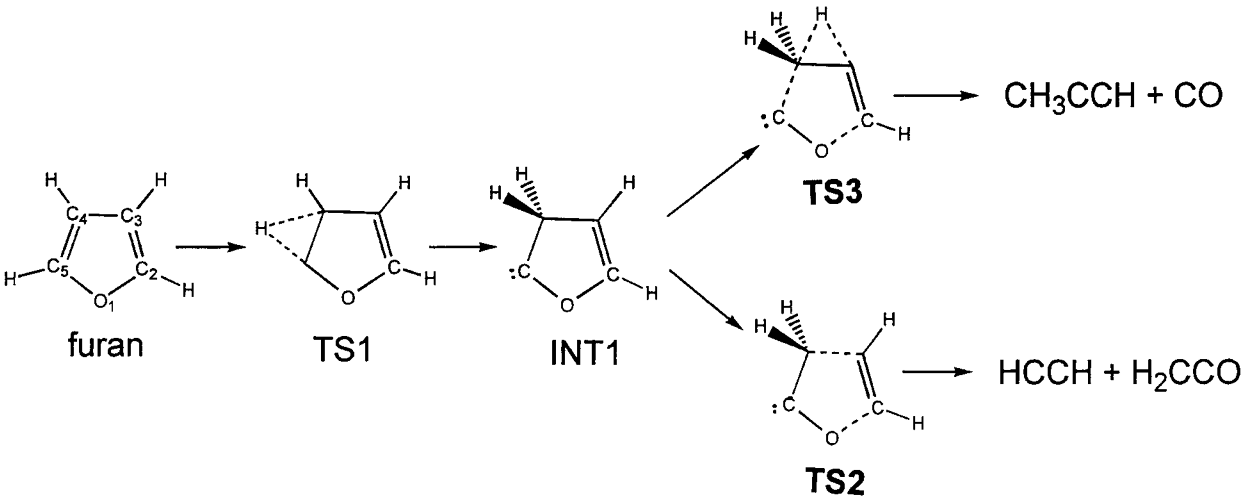

SCHEME 3. Proposed unimolecular decomposition channel of furan similar to that of isoxazole proposed in a recent experimental study.[5]

the proposed decomposition channels (Schemes 3–5) of furan.

Computational Details

All our calculations were carried out using the Gaussian-94 program package.[7] The equilibrium and transition structures described in Schemes 3–5 were fully optimized by Becke's three-parameter hybrid DFT/HF method[8] using the Lee–Yang–Parr correlation functional[9] (B3LYP) and the 6-31G** basis set.[10] This method has been shown to give reliable structures for molecules consisting of the first-row atoms.[11] Vibrational analyses were carried out, at the same level of theory, to characterize the optimized structures as equilibrium or transition states. Intrinsic reaction coordinate (IRC)[12] calculations were performed on the transition structures to make sure the transition states connect the desired reactants and products. Energies of the optimized structures were evaluated at the B3LYP/6-31G** structures by MP4(SDQ)(FC)/6-311++G**, QCISD/6-311++G**, and QCISD(T)/6-311++G**. Zero-point vibrational energies (ZPE) were taken into account and were approximated by one-half of the sum of B3LYP/6-31G** harmonic frequencies.

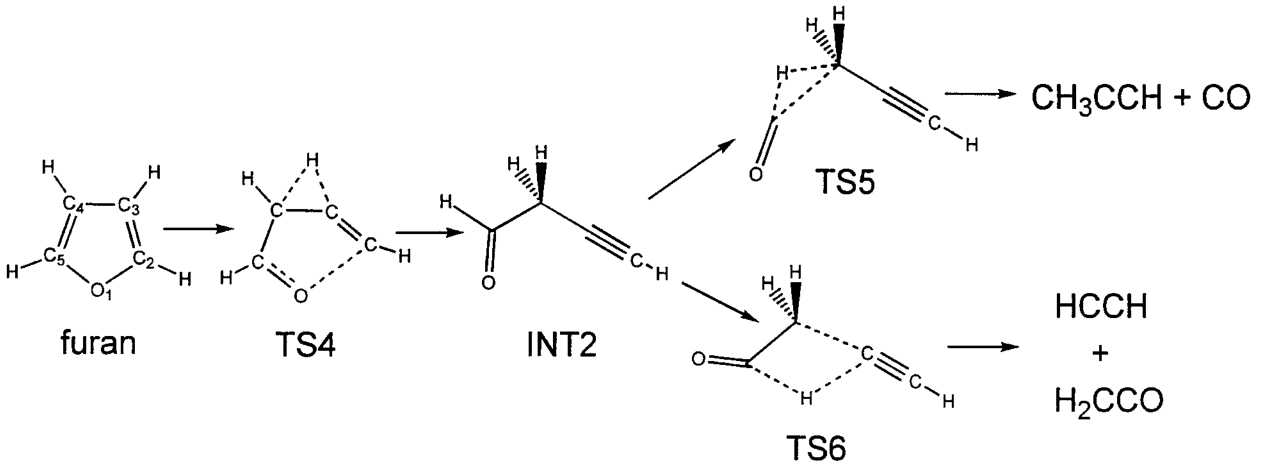

SCHEME 4. Proposed unimolecular decomposition channel of furan similar to that of isoxazole proposed in a recent theoretical study.[6]

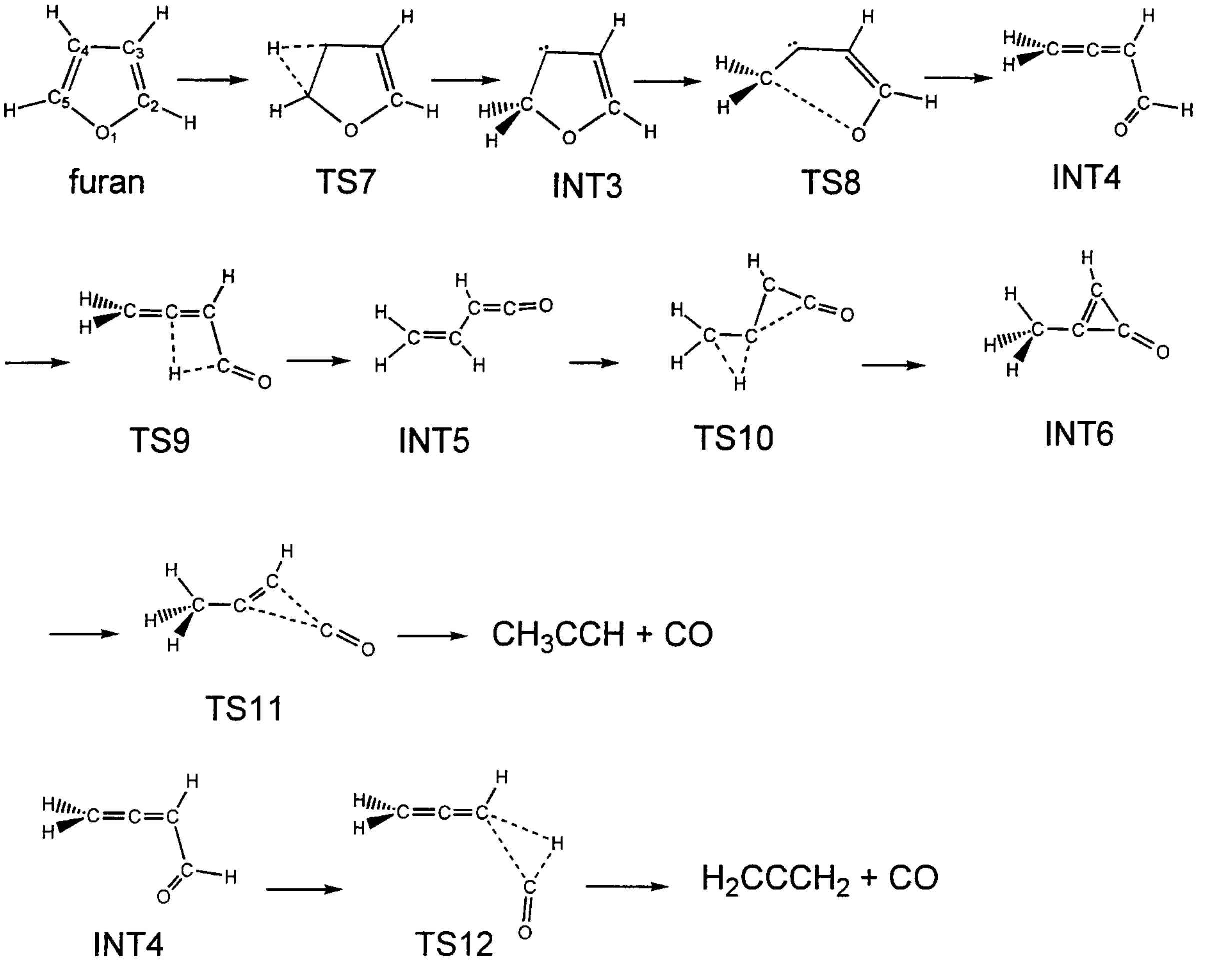

SCHEME 5. Unimolecular decomposition channel of furan proposed in the present study.

Results and Discussion

Prominent geometrical parameters of the equilibrium and transition state structures depicted in Schemes 3–5, fully optimized by B3LYP/6-31G**, are presented in Figure 1. In the figure, bond lengths are given in angstroms and angles in degrees. Available experimental structural parameters of furan are also presented in Figure 1 for comparison. We carefully searched literature on the proposed stable intermediates **INT2**, **INT4**, **INT5**, and **INT6**, but failed to find any experimental structural data to compare with the calculated results. The experimental data of furan were derived from microwave spectra[13] and are in good agreement with the calculated results. The largest difference between the calculated and microwave bond distances was 0.005 Å, and the largest differences in bond angles was 0.6°. This accuracy is

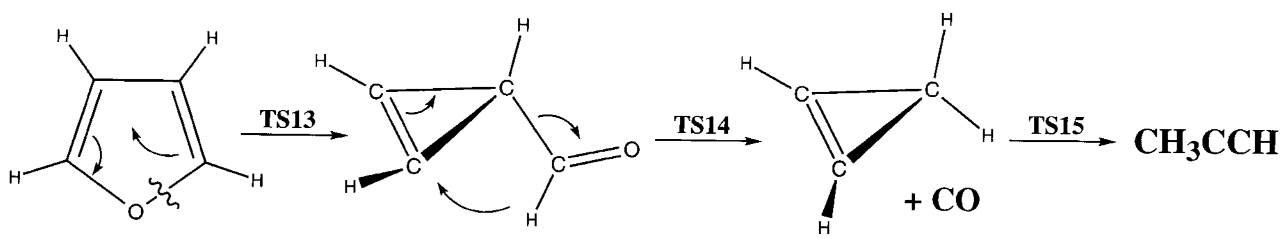

SCHEME 6

typical of B3LYP for equilibrium structures of compounds consisting of first-row atoms.[11] We hope that the method is equally reliable for transition states.

Because of its aromatic nature, the chemical bonds of the furan ring are quite strong. Thus, the formation of **INT1** goes through a very tight transition state, **TS1**, with a small change in the ring structure. Starting from **INT1**, the formation of $H_2C{=}C{=}O + HC{\equiv}CH$ goes through a transition state, **TS2**, of concerted C—O and C_2—C_4 bond cleavage, while the formation of $CH_3C{\equiv}CH$ + CO goes through a concerted transition state, **TS3**, of hydrogen migration from C_4 to C_3 in addition to C_2—C_3 and C—O bond cleavage. Because of the additional energy requirement for hydrogen migration, **TS3** is expected to be higher in energy than **TS2**. Therefore, if the decomposition reaction goes through Scheme 3, $H_2C{=}C{=}O$ and $HC{\equiv}CH$ are expected to be major products.

The first transition state of Scheme 4 (**TS4**) is a transition state of C—O bond cleavage and hydrogen migration from C_3 to C_4. This transition state is highly asynchronous as the breaking C—O bond distance is already 3.7 Å, while the migrating hydrogen is still closer to the carbon atom it originally bonded to. The unusually long C—O distance results from the formation of a *sp*-hybridized carbon with hydrogen migration. From the unusually long C—O distance, it looks like the formation of **INT2** is a stepwise process with the C—O bond breaks first followed by hydrogen migration. However, our careful search for an intermediate failed and our IRC analysis indicates that **TS4** is indeed the only transition state for the formation of **INT2** from furan. It is a highly asynchronous but concerted transition state.

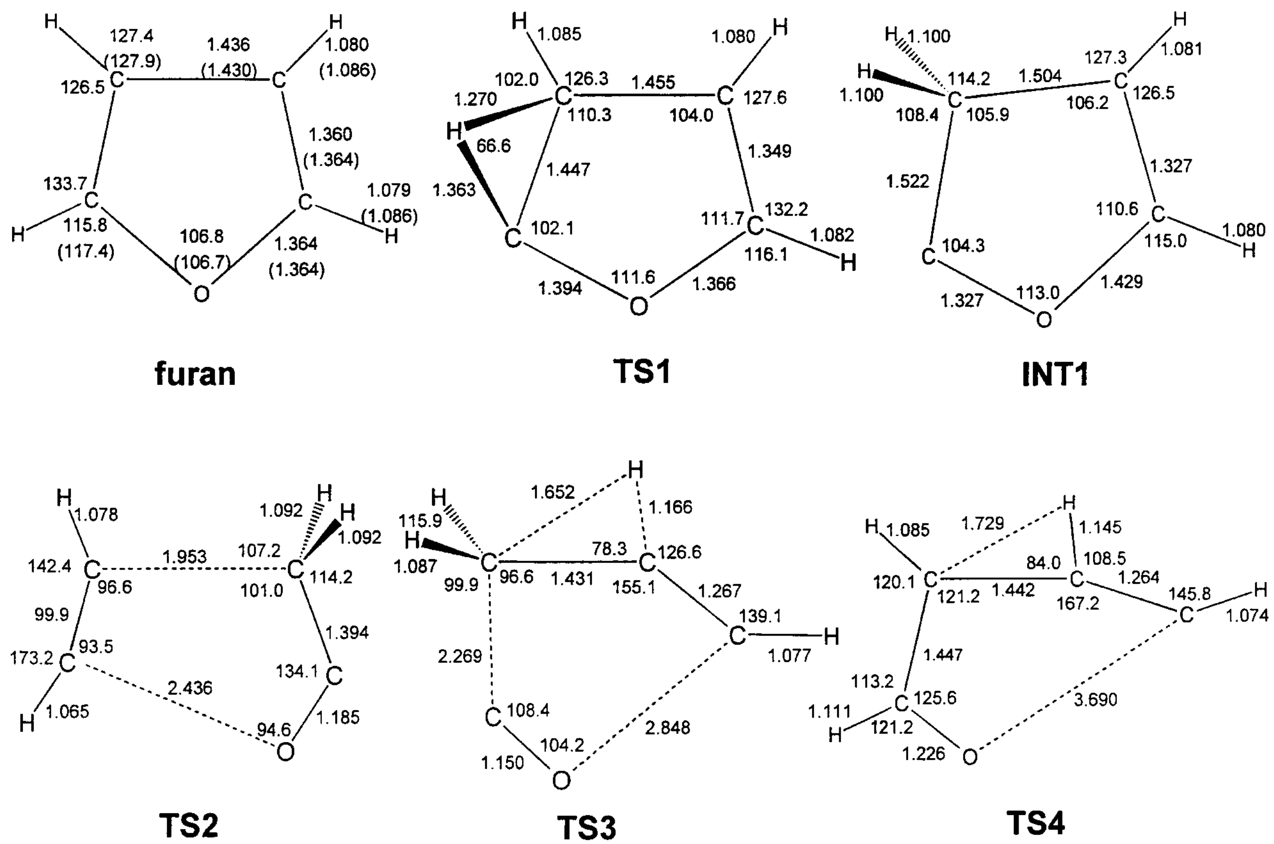

FIGURE 1. (A, B, C) Prominent B3LYP / 6-31G** geometrical parameters of the equilibrium and transition state structures of the proposed unimolecular decomposition pathways of furan. Bond lengths are given in angstroms and angles in degrees. Refer to Schemes 3, 4, and 5 for the structures presented. Numbers in parentheses are microwave structural parameters of furan[13]. (B) and (C) are on pages xxx and xxx.

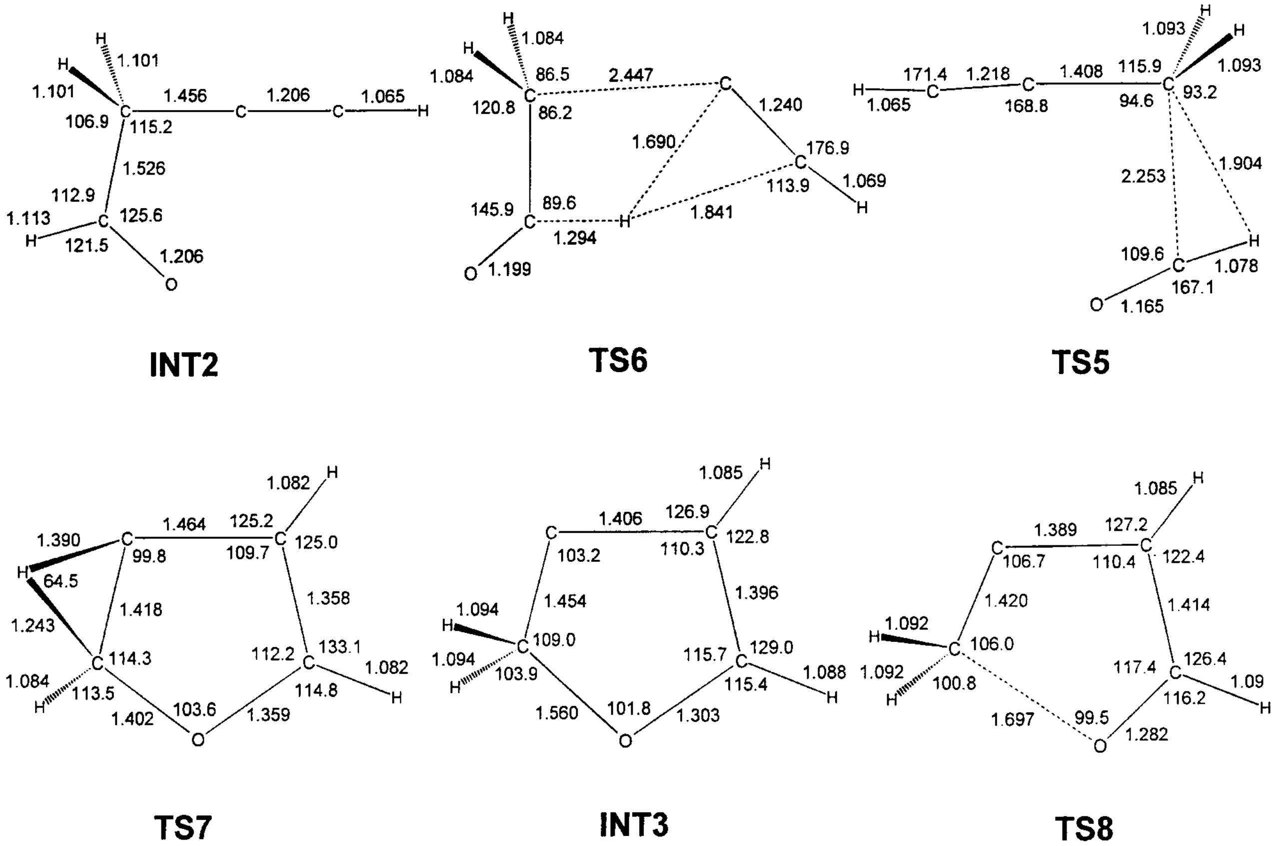

FIGURE 1. (Continued)

Starting from **INT4**, the reaction leading to $CH_3C{\equiv}CH + CO$ goes through a three-membered transition state **TS5** for C—C bond cleavage coupled with hydrogen transfer, while the formation of $H_2C{=}C{=}O + HC{\equiv}CH$ goes through a four-membered transition state **TS6** for C—C bond cleavage and hydrogen transfer.

Along Scheme 5, furan first goes through a tight transition state, **TS7**, for hydrogen transfer to form intermediate **INT3**. **TS7** is very similar to **TS1**, but they differ in the direction of the hydrogen migration. They are very close in energy. **INT3** has a very long C—O bond of 1.56Å, which is very easily broken to form an open-chain intermediate, **INT4**. The transition state for ring opening, **TS8**, is about 1 kcal/mol higher in energy than **INT3**. Considering that **TS7** is more than 10 kcal/mol higher than **INT3**, the excess thermal energy in **INT3** will easily open the ring and form **INT4**. Thus, **INT3** is expected to be a very short-lived intermediate. **INT4** is a relatively stable intermediate. It can decompose by breaking the C—C single bond coupled by a hydrogen transfer from the carbonyl carbon to one of the other three carbon atoms. If the hydrogen transfers to the terminal carbon atom in **INT4**, $CH_3C{\equiv}CH$ and CO are produced. If it transfers to the carbon atom in the middle, **INT5** is produced. If the hydrogen transfers to the carbon adjacent to the carbonyl group, $H_2C{=}C{=}CH_2$ and CO are formed. We performed a careful search of transition states for all three possibilities, but failed to find the transition state for hydrogen transfer to the terminal carbon atom. All attempts to locate this transition state converged to **TS9**, the transition state for hydrogen transfer to the middle carbon atom. Because of the high energy requirement for bending the $C{=}C{=}C$ moiety, we suspect the existence of a transition state for hydrogen transfer to the terminal carbon atom. On the other hand, even if the transition state exists it may be high in energy and cannot compete with **TS9**. For hydrogen transfer to the adjacent carbon, a transition state, **TS12**, is located, which is about 110 kcal/mol (without

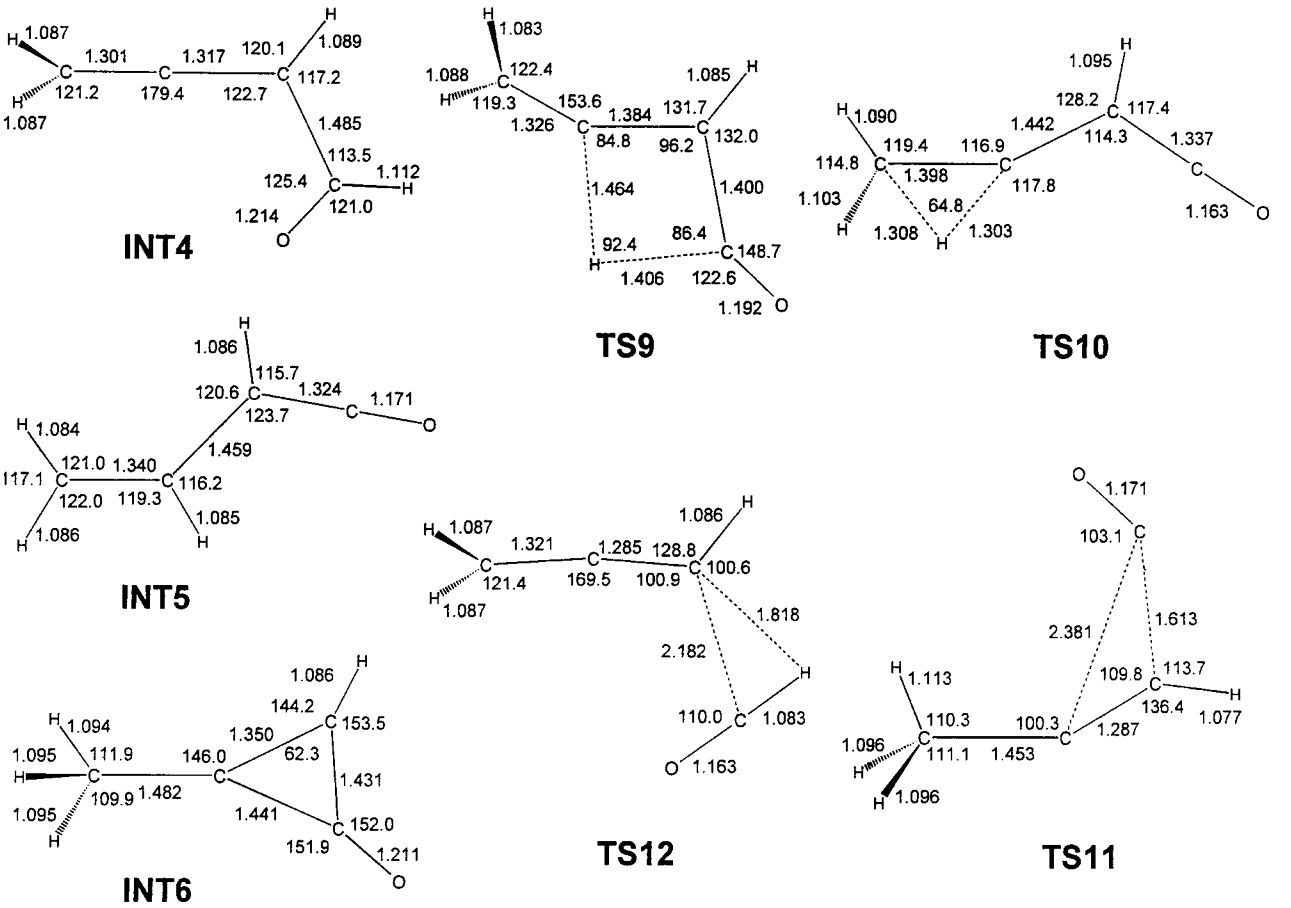

FIGURE 1. (Continued)

ZPE correction, about 100 kcal/mol with ZPE correction) higher than furan. The activation energy derived from experimental data for the formation of $H_2C{=}C{=}CH_2$ is 105 kcal/mol,[4] indicating that the theoretical results are reasonably reliable.

At the B3LYP/6-31G** level of theory, **TS9** is only 81.1 kcal/mol higher in energy than furan. Therefore, formation of **INT5** is much more favorable than formation of $H_2C{=}C{=}CH_2$ and CO. **INT5** can have another hydrogen transfer via transition state **TS10** to form intermediate **INT6**. **TS10** and **TS9** are very close in energy, but they are separated by a quite stable intermediate, **INT5**. Once **INT6** is formed, it can decompose easily through transition state **TS11** to produce $CH_3C{\equiv}CH + CO$.

Relative energies of the equilibrium and transition state structures for decomposition via Schemes 3–5 calculated by B3LYP/6-31**, MP4(SDQ)/6-311+ + G**, QCISD/6-311+ + G**, and QCISD(T)/6-311++G**, at the B3LYP/6-31G** structures, are presented in Table I. In this table, the total electronic energy of furan is given in hartrees. The energies of all other structures are given in kilocalories per mole relative to furan. Zero-point vibrational energies (ZPE), approximated by one half of the sum of B3LYP/6-31G** harmonic frequencies, are also given in this table. Relative energies along Schemes 3–5 calculated by QCISD(T)/6-311++G** plus ZPE correction are also presented schematically in Figures 2 and 3. They show that among the three unimolecular decomposition channels considered, the most favorable one for producing $CH_3C{\equiv}CH$ and CO is Scheme 5. The highest activation energy along this channel is 77.0 kcal/mol, which occurs at **TS9**. **TS10** is very close in energy to **TS9**, but they are separated by intermediate **INT5**, which is 66 kcal/mol lower in energy. The activation energy for $CH_3C{\equiv}CH$ formation derived from the ex-

perimental data is 77.5 ± 2.5 kcal/mol,[4] and in good agreement with the calculated result. Schemes 3 and 4 also give $CH_3C{\equiv}CH + CO$ as possible products. However, for the reaction to produce $CH_3C{\equiv}CH$ and CO, Scheme 4 has an activation energy of 95.6 kcal/mol, and Scheme 4 has an activation energy of 100.9 kcal/mol. Therefore, neither Scheme 3 nor Scheme 4 can compete with Scheme 5 in the production $CH_3C{\equiv}CH$ and CO.

Schemes 3 and 4 also produce $H_2C{=}C{=}O$ and $HC{\equiv}CH$. For this to occur, Scheme 3 has an activation barrier (at **TS2**) of 80.3 kcal/mol, whereas Scheme 5 has an activation barrier (at **TS6**) of 153.4 kcal/mol. Thus, among the decomposition channels considered, Scheme 3 is more favorable for the formation of $H_2C{=}C{=}O$ and $HC{\equiv}CH$. The activation energy for $HC{\equiv}CH$ formation derived from experimental data is 77.5 kcal/mol,[4] which compares reasonably with the calculated activation energy due to **TS2**. These results indicate that Scheme 3 is probably the unimolecular decomposition channel for $HC{\equiv}CH$ formation, and Scheme 5 is a reasonable unimolecular decomposition channel for $CH_3C{\equiv}CH$ formation. Scheme 4, the likely major decomposition channel for isoxazole,[6] is a much less competitive decomposition channel of furan.

Although the calculated highest activation energy of Scheme 3 is about 3 kcal/mol higher than that of Scheme 5, the rate of decomposition along Scheme 3 could compete with the rate of decomposition along Scheme 5. This is because **INT5** is a quite stable intermediate along Scheme 5. Under the experimental conditions, **INT5** may lose its excess thermal energy by collisional deactivation. When this occurs, additional energy is required for **INT5** to overcome the next barrier peaked at **TS10**.

A reviewer kindly pointed out that Scheme 6 is also a reasonable unimolecular decomposition pathway of furan, as the first step is known in the photochemistry of furan and the second step is Woodward–Hoffmann allowed. To examine the feasibility of this mechanism, we have optimized the transition structures **TS13** and **TS14** by B3LYP/6-31G**. At this level of theory, **TS13** is 86.9 kcal/mol higher than furan, and **TS14** is 98.2 kcal/mol higher than furan. At the same level of

TABLE I.
Energies[a] of Equilibrium and Transition State Structures[b] of the Proposed Decomposition Channels[c] of Furan.

		Scheme 3						Scheme 4			
Method[d]	Furan	**TS1**	**INT1**	**TS2**	**TS3**	$H_2CCO + HCCH$	$CH_3CCH + CO$	**TS4**	**INT2**	**TS5**	**TS6**
B3LYP	−230.02737	70.5	58.4	92.8	116.1	60.1	36.7	104.3	36.9	112.6	166.8
MP4SDQ	−229.45936	68.8	54.4	91.2	108.6	51.8	19.6	107.0	28.5	110.1	169.4
QCISD	−229.46021	68.5	53.5	91.4	108.2	51.6	19.6	106.2	28.4	110.7	166.1
QCISD(T)	−229.49453	68.1	54.4	86.1	104.1	52.8	21.9	100.8	29.9	107.3	163.1
ZPE[e]	44.0	40.5	42.0	38.3	35.6	36.6	38.0	37.1	40.9	37.6	34.3
QCISD(T) + ZPE		64.6	52.4	80.3	95.6	45.5	15.9	93.8	26.8	100.9	153.4

	Scheme 5										
Method[d]	**TS7**	**INT3**	**TS8**	**INT4**	**TS9**	**INT5**	**TS10**	**INT6**	**TS11**	**TS12**	$H_2CCCH_2 + CO$
B3LYP	74.2	59.5	59.8	27.1	81.1	14.2	84.2	32.4	59.6	108.4	33.8
MP4SDQ	72.2	59.4	61.8	26.5	86.4	12.6	82.4	32.4	59.2	110.5	21.9
QCISD	71.9	58.3	60.5	26.1	86.8	12.9	82.5	32.5	59.5	110.8	21.7
QCISD(T)	71.5	58.0	59.2	26.9	83.2	13.5	82.6	33.4	53.8	107.2	23.7
ZPE[e]	40.8	42.3	41.7	41.2	37.9	41.6	38.3	41.6	49.5	37.5	37.9
QCISD(T) + ZPE	68.2	56.4	56.9	24.0	77.0	11.1	76.8	31.0	49.5	100.7	17.6

[a] The total energy of furan is given in hartrees, the energies of all other structures are given in kilocalories per mole relative to that of furan.
[b] The structures were optimized by B3LYP/6-31G** and are given in Figure 1.
[c] The decomposition channels are described in Schemes 3, 4, and 5.
[d] The B3LYP results were obtained using the 6-31G** basis set. The MP4SDQ, QCISD, and QCISD(T) results were obtained with the 6-311++G** basis set.
[e] Zero-point vibrational energy (kcal/mol) approximated by one half of the sum of B3LYP/6-31G** harmonic frequencies.

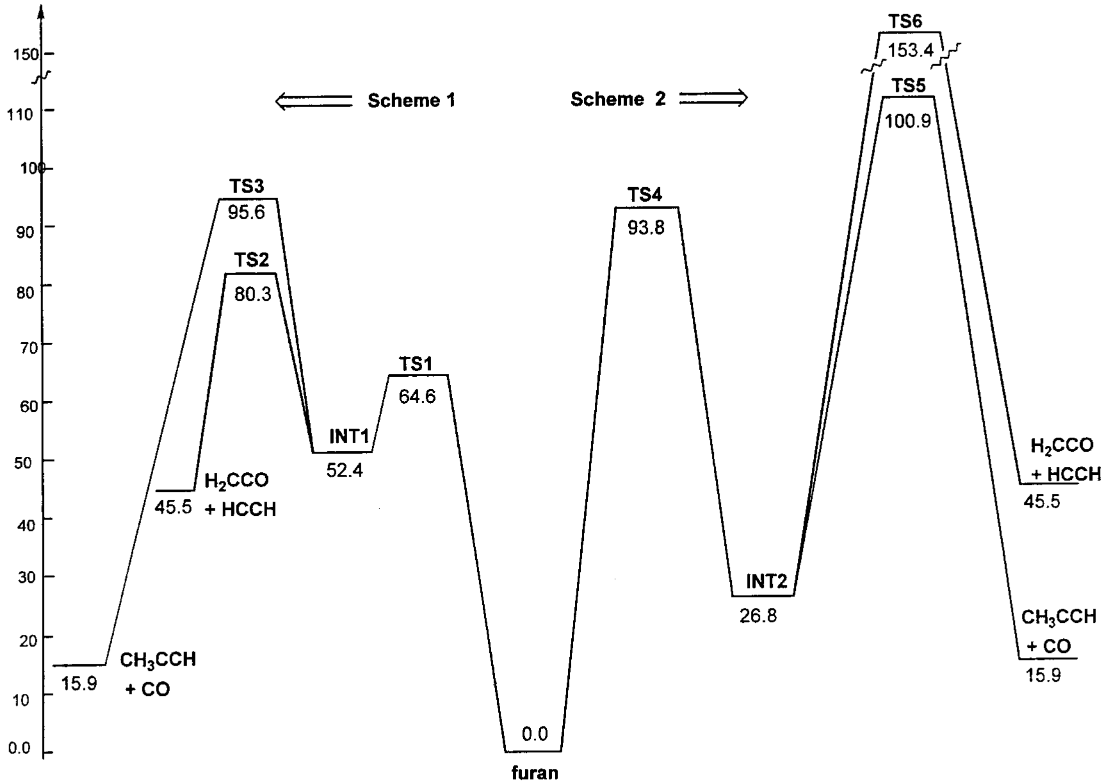

FIGURE 2. Energy profiles for furan decomposition along Schemes 3 and 4 evaluated by QCISD(T)/6-311++G** plus ZPE correction. The energies given are in kilocalories per mole relative to that of furan.

theory, the highest barrier of Scheme 3 leading to ketene and acetylene is 92.8 kcal/mol (**TS2**), and the highest barrier along Scheme 5 is 84.2 kcal/mol (**TS10**). Single-point MP4(SDQ)/6-311++G** calculation on **TS14** shows that it is 100.9 kcal/mol higher than furan without ZPE correction, and 94.2 kcal/mol higher with ZPE correction. At the MP4(SDQ)/6-311++G**//B3LYP/6-31G** level, the highest barrier along Scheme 3 is 91.2 kcal/mol without ZPE and 85.5 kcal/mol with ZPE. The highest barrier along Scheme 5 is 86.4 kcal/mol without SPE and 80.3 kcal/mol with ZPE. The results indicate that the mechanism just described is less favorable than Schemes 3 and 5, and that the mechanisms of photo and thermal decompositions may be different.

Summary

Density functional theory and *ab initio* calculations were performed to investigate three unimolecular decomposition channels of furan. All critical structures of the proposed decomposition channels were fully optimized by B3LYP/6-31G** and characterized by vibrational and intrinsic reaction coordinate analyses. Single-point energy calculations were carried out at theoretical levels up to QCISD(T)/6-311++G**. On the basis of the calculated results, it is concluded that the unimolecular decomposition channel of isoxazole, proposed in an experimental study and implied to be the main decomposition channel of furan, is probably responsible only for the formation of $HC{\equiv}CH$ and $H_2C{=}C{=}O$, minor products of furan thermal decomposition. A new decomposition mechanism proposed in the present study was shown to be more likely responsible for the formation of $CH_3C{\equiv}CH$ and CO, major products of furan thermal decomposition. Although furan is isoelectron with isoxazole, the favorable decomposition channel for isoxazole proposed in our recent theoretical study was shown to be less competitive for furan than the other two decomposition channels examined.

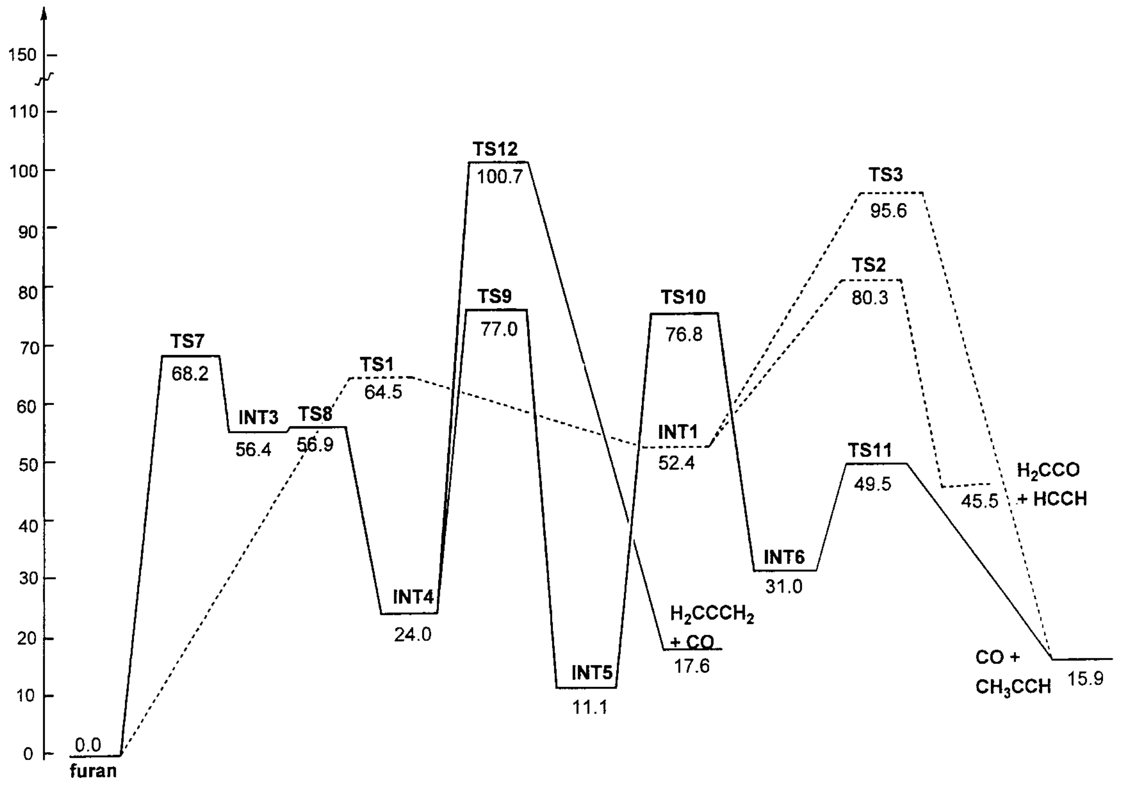

FIGURE 3. Energy profiles for furan decomposition along Scheme 3 (broken line) and Scheme 5 (solid line) evaluated by QCISD(T) / 6-311++G** plus ZPE correction. The energies given are in kilocalories per mole relative to that of furan.

References

1. J. P. Longwell, In *Alternate Hydrocarbon Fuels: Combustion and Chemical Kinetics*, C. T. Bowman and J. Birkeland, Eds., American Institute of Aeronautics and Astronautics, New York, 1978.
2. J. H. Lee and I. N. Tang, *J. Chem. Phys.*, **77**, 4459 (1982).
3. J. E. Sickles, L. A. Ripperton, W. C. Eaton, and R. S. Wright, *Environmental Protection Agency Publication EPA-600 / 7-78-029, EPA*, Washington, DC, 1978.
4. A. Lifshitz, M. Bidani, and S. Bidani, *J. Phys. Chem.*, **90**, 5373 (1986).
5. A. Lifshitz and D. Wohlfeiler, *J. Phys. Chem.*, **96**, 4505 (1992).
6. J. Higgins, X. Zhou, and R. Liu, *J. Phys. Chem.*, in press.
7. M. J. Frisch, G. W. Trucks, H. B. Schlegel, P. M. W. Gill, B. G. Johnson, M. A. Robb, J. R. Cheeseman, T. Keith, G. A. Petersson, J. A. Montgomery, K. Raghavachari, M. A. Al-Laham, V. G. Zakrzewski, J. V. Ortiz, J. B. Foresman, J. Cioslowski, B. B. Stefanov, A. Nanayakkara, M. Challacombe, C. Y. Peng, P. Y. Ayala, W. Chen, M. W. Wong, J. L. Andres, E. S. Replogle, R. Gomperts, R. L. Martin, D. J. Fox, J. S. Binkley, D. J. Defrees, J. Baker, J. P. Stewart, M. Head-Gordon, C. Gonzalez, and J. A. Pople, *Gaussian 94, Revision B.1*, Gaussian, Inc., Pittsburgh, PA, 1995.
8. A. D. Becke, *J. Chem. Phys.*, **98**, 5648 (1993).
9. C. Lee, W. Yang, and R. G. Parr, *Phys. Rev.* **B37**, 785 (1988); B. Miehlich, A. Savin, H. Stoll, and H. Preuss, *Chem. Phys. Lett.*, **157**, 200 (1988).
10. W. J. Hehre, R. D. Ditchfield, and J. A. Pople, *J. Chem. Phys.*, **56**, 2257 (1972).
11. B. Ma, J-H. Lii, H. F. Schaefer III, and N. L. Allinger, *J. Phys. Chem.*, **100**, 8763 (1996).
12. C. Gonzalez and H. B. Schlegel, *J. Phys. Chem.*, **94**, 5523 (1990).
13. P. Nosberger, A. Bauder, and H. H. Gunthard, *Chem. Phys.*, **1**, 418 (1973).